crystals

MDPI

*Letter*

# Switchable Two-Dimensional Liquid Crystal Grating in Blue Phase

**Bing-Yau Huang [1], Shih-Hung Lin [2], Ke-Chin Lin [1] and Chie-Tong Kuo [1,*]**

[1] Department of Physics, National Sun Yat-sen University, Kaohsiung 80424, Taiwan; flyfish31@hotmail.com (B.-Y.H.); z7824054@gmail.com (K.-C.L.)

[2] Department of Optometry, Chung Shan Medical University, Taichung 40201, Taiwan; shihhung@csmu.edu.tw

* Correspondence: ctkuo@mail.nsysu.edu.tw; Tel.: +886-7-525-3727

Received: 11 May 2017; Accepted: 19 June 2017; Published: 21 June 2017

**Abstract:** We demonstrate a switchable two-dimensional phase grating in blue phase liquid crystal (BPLC), which is fabricated by sawtooth in-plane-switch (IPS) electrodes. They are used to generate the horizontal electric field on a single indium-tin-oxide (ITO) glass substrate and, as a result, the 1-D and 2-D phase gratings can be mutual switched via different polarizations of incident light with an applied voltage. The first-order diffraction efficiency is up to 20% and 10% for the 1-D and 2-D phase grating at $V$ = 150 V, respectively. Moreover, the rise and decay time is 0.9 and 1.1 ms, respectively, which is suitable for wide applications of high-speed optical manipulations.

**Keywords:** in-plane-switch sawtooth electrode; blue phase liquid crystal

## 1. Introduction

Electrically tunable one-dimensional (1-D) liquid crystal (LC) grating has been widely used for beam steering [1], optical fibers [2], and three-dimensional displays [3]. Since the requirement of multi-beam interactions, the grating with two-dimensional (2-D) diffraction has drawn much attention for the application of beam multiplexing [4]. The LC diffraction grating, first reported by Carroll [5], requires a periodical refractive index distribution of LC inside the cell. To achieve such a distribution, various methods have been proposed. First, a special electrode configuration, such as interdigitated (or in-plane-switch, IPS) electrodes, is designed to produce a non-uniform electric field for fabricating the LC phase grating [6–12]. Other ways of generating the periodicity of the refractive index are through the reorientation of the LC molecular director using photoalignment [13,14], and the holographic technique [15,16]. In addition, a phase grating based on Methyl Red-doped LC has been demonstrated by Gau et al. with multiple holographic recordings [17]. One- and two-dimensional (1-D and 2-D) phase gratings can be achieved in one position by using the angular and spatial multiplexing technique. Senyuk et al. demonstrated a 1-D/2-D switchable grating which utilizes the undulation in the layer of cholesteric LC (CLC) to form the grating profile [18]. Another electrically switchable grating has been reported by using the field-induced 2-D pattern in polymer-stabilized CLC [4]. However, these gratings have inherent problems, including low diffraction efficiency and slow response time, as reported in previous studies.

Blue phase liquid crystal (BPLC) has been developed recently for optoelectronic applications in photonics, light modulation, and displays [19–22], because of its unique characteristics including a fast response time and no requirement for an alignment layer. Under an external electric field, the Kerr effect is exhibited by local reorientation of the LC directors and electrostriction in BPLC [23]. Based on these properties, the phase grating in BPLC has been investigated in recent years. A polarization dependence of BPLC phase grating has been demonstrated on an IPS electrode [24], which possesses

high diffraction efficiency and a fast response time for the transverse-magnetic (TM) polarization of the probe beam.

In this study, according to the polarization dependence of BPLC phase grating on a horizontal electric field generated by an IPS electrode, a switchable two-dimensional BPLC grating is proposed through different polarizations of incident light with the sawtooth IPS electrode on a single indium-tin-oxide (ITO) glass substrate. The interchange between 1-D and 2-D grating can be easily attained only by changing the polarization of the incident beam. In addition, this device shows good results in diffraction efficiency and response time.

## 2. Results and Discussion

An image of the BPLC mixture under optical polarized microscope (OPM) is shown in Figure 1a. The domain size is more than 50 μm, and the great lattice size of BPLC can validly reduce the scattering effect when the incident light passes through the grating cell. Figure 1b–d show the OPM images of the BPLC grating at various voltages with crossed polarizers, which are taken by using the irradiation of unpolarized red light (λ = 632.8 nm). At $V$ = 0 V, the fact that the BPLC grating presents a pure dark state indicates that the grating is in an optically isotropic state, as shown in Figure 1b. When the voltage is increased to 70 V, little transmittance is observed at the edge of the sawtooth electrode because of the birefringence of BPLC induced by the fringing field, as shown in Figure 1c. When the applied voltage continues rising to 150 V, high transmittance is observed in the gap between electrodes and at the edge of the electrodes because of the birefringence of BPLC induced by the horizontal electric field in the crossing of electrode gaps, leading to a change in the refractive index, as shown in Figure 1d. However, the fact that no phase retardation occurs on the top of the electrodes suggests that the transmittance has vanished.

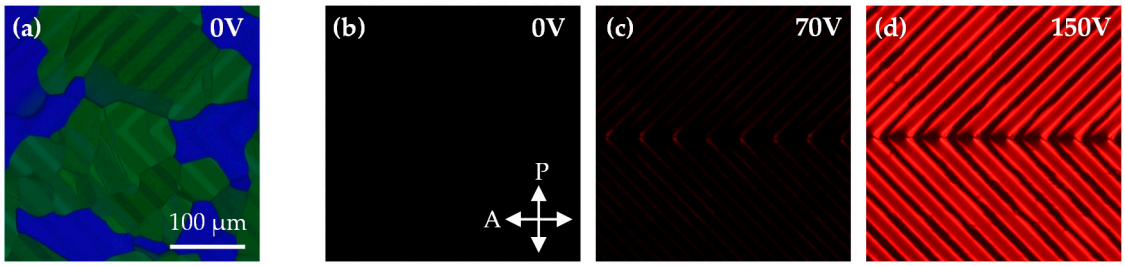


**Figure 1.** (**a**) The mixture of blue phase in the voltage-off state; (**b**–**d**) The optical polarized microscope images of the BPLC grating under the irradiation of red light (λ = 632.8 nm) at various voltages; $V$ = 0, 70, and 150 V, respectively.

The geometric orientation for the polarization of incident light and the sawtooth electrode is shown in Figure 2a. The polarizations of incident light parallel to the $x$-axis and $y$-axis are defined as 0° and 90°, respectively. The direction perpendicular to the bisector between the positive $x$-axis and the positive $y$-axis is defined as 45°. When the linearly polarized light is parallel to one side of the sawtooth electrode, that it, one is perpendicular to the other (e.g., 0° or 90°), it experiences the periodic phase distribution of $n_{iso}/n_e(E)$ on the perpendicular side and that of $n_{iso}/n_o(E)$ on the parallel side. $n_e(E)$ and $n_o(E)$ represent the effective refractive index of BPLC in the directions parallel and perpendicular to the electric field, which can be expressed as Equations (1) and (2):

$$n_e(E) = n_{iso} + \frac{2\delta n_{ind}(E)}{3} \quad (1)$$

$$n_o(E) = n_{iso} - \frac{\delta n_{ind}(E)}{3} \quad (2)$$

where $\delta n_{ind}(E)$ is the birefringence of BPLC induced by the electric field. The induced birefringence

can be obtained by the extended Kerr effect [25]:

$$\delta n_{ind}(E) = \delta n_{sat}\left\{1 - \exp\left[-\left(\frac{E}{E_s}\right)^2\right]\right\} \quad (3)$$

Here, $\delta n_{sat}$ presents the saturated index change and $E_s$ is the saturation field. As a result, the incident light on the perpendicular side has more phase change ($\delta n_e(E) = n_e(E) - n_{iso}$) than on the parallel side ($\delta n_o(E) = n_{iso} - n_o(E)$), which leads to the formation of a 1-D grating. Figure 2b,d show the diffraction patterns of the 1-D grating with the polarization of 0° and 90° of incident light at $V$ = 150 V, respectively. A blurry diffraction pattern is hardly observed in the direction perpendicular to the first order diffraction pattern. Compared with the intensity of the first order diffraction, this blurry diffraction can be neglected. As the linearly polarized light intersects with both sides of the sawtooth electrode by 45°, the periodic phase distribution of both sides of the sawtooth electrode interact. Thus, the diffraction pattern of the 2-D grating can be produced, as shown in Figure 2c.

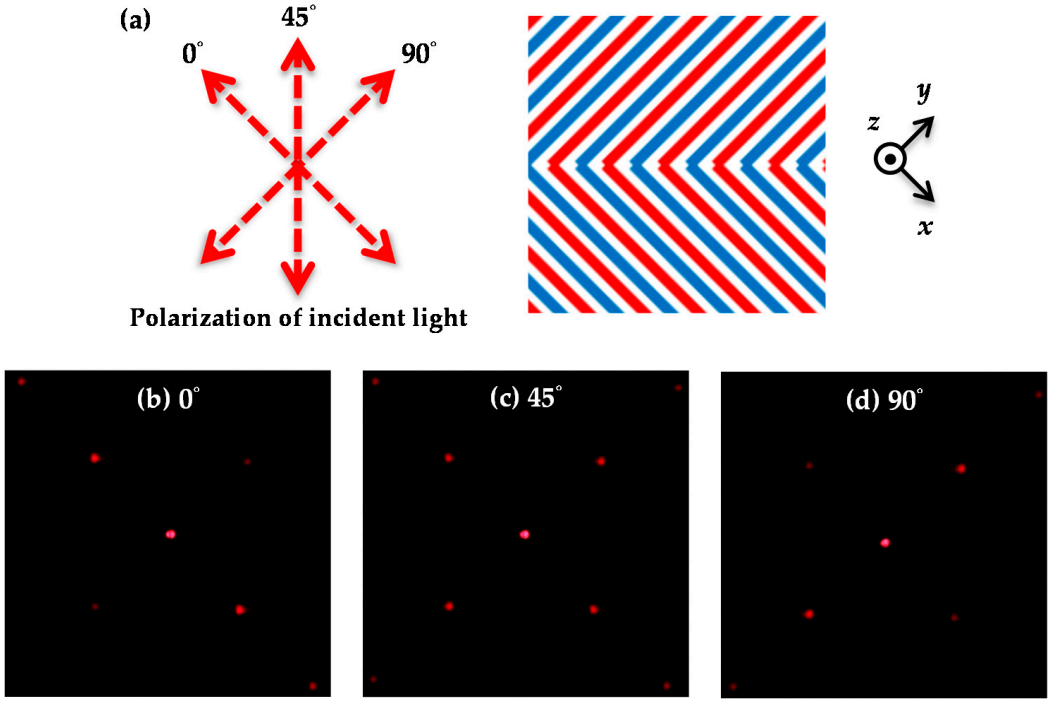


**Figure 2.** (**a**) The schematic diagram for the polarization of incident light and the sawtooth electrode; The diffraction patterns of 1-D/2-D grating with the polarization of (**b**) 0°, (**c**) 45°, and (**d**) 90° of incident light at $V$ = 150 V.

Additionally, the zeroth and first order diffraction efficiencies for the 1-D/2-D BPLC grating are measured, as shown in Figure 3. The diffraction efficiency is defined as the ratio of the intensity between the $N$th order diffraction and the incident light passing through the cell at $V$ = 0 V by Equation (4):

$$\eta_N(V) = \frac{I_N(V)}{I_0}. \quad (4)$$

In the voltage-off state, the first order diffraction efficiency is very small (~0.3%) for both the 1-D and 2-D gratings, and is contributed by the sawtooth electrode. As the voltage increases, the zeroth order diffraction efficiency decreases, whereas the first order diffraction efficiency increases immediately. This suggests that a small threshold voltage is required for the BPLC grating. At $V$ = 150 V, the first order diffraction efficiencies can approach to 20% and 10% for the 1-D and 2-D phase gratings, respectively. The first order diffraction efficiency for the 2-D grating is nearly

half that of the 1-D grating. The theoretical diffraction efficiency can be obtained via the calculated phase modulation in blue phase grating. The phase modulation with the induced refractive indices is described by Equation (5):

$$\phi(x,y) = \int_0^d \delta n_{ind}(E(x,y,z))dz, \quad (5)$$

where $d$ is the cell gap, $z$ is the surface normal to the substrate, and $x$, $y$ are indicated in Figure 2. The maximal diffraction efficiency of the proposed switchable grating occurs at the applied voltage of 150 V. The high operating voltage of the BPLC grating can be further reduced by using the high Kerr constant of LC or IPS electrode design [26–29].

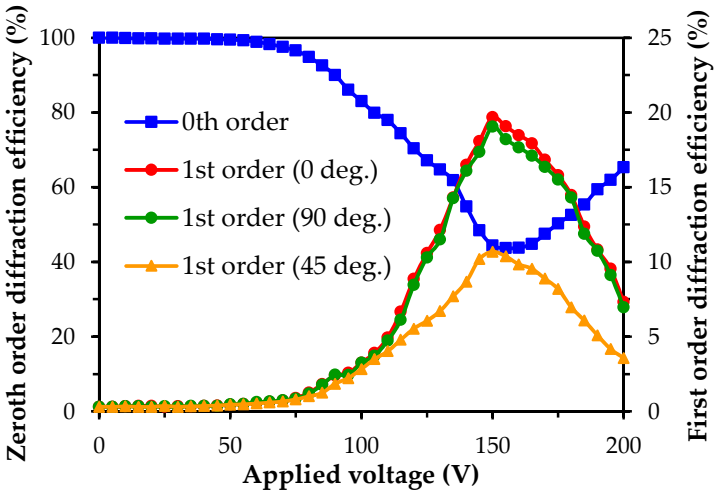


**Figure 3.** The zeroth and first order diffraction efficiencies for 1-D and 2-D BPLC gratings.

The hysteresis curves of the first order diffraction efficiency for the 1-D and 2-D BPLC gratings are depicted in Figure 4. The solid and dashed lines are represented for the forward and backward driving, respectively. The hysteresis affects the accuracy of the control on grayscale in BP applications, which causes different transmittance even at the same voltage during the process of increasing/descending voltage. The hysteresis generally occurs in blue phase I (BPI) for lattice distortion as the applied voltage reaches above the threshold [30]. In this experiment, the hysteresis is defined as the difference in voltage between the forward and backward driving at the half maximum of diffraction efficiency. The results show that the hysteresis ($\Delta V_{50}$) of the first order diffraction efficiency is ~10 V for 1-D and 2-D BPLC gratings, which corresponds to ~6.67% of the voltage of maximum diffraction efficiency ($V_{\max}$ ~150 V). The small hysteresis observed is due to the large domain size (over 50 μm) of the BPLC sample [31], and the operating temperature of the BPLC grating is close to the temperature of phase transition between BPI and blue phase II (BPII) (~45.5 °C) [30]. However, a method can be utilized to reduce the hysteresis, such as using the BPLC sample with a temperature in the BPII range [30], polymer stabilized blue phase liquid crystal (PSBPLC) [32–34], and elliptical protrusion electrodes [35]. The measurement of response time for the first order diffraction intensity of the 1-D BPLC grating is shown in Figure 5. The time interval of variation in the first order diffraction intensity from 10% to 90% is defined as the rise time, and from 90% to 10% it is defined as the decay time. According to the results, the rise time is 0.9 ms and the decay time is 1.1 ms. The response time for the proposed BPLC gratings is in the sub-millisecond range, which is faster than that for the general LC grating. The response time can be further reduced by changing the BPLC to the PSBPLC [36]. However, the driving voltage of a PSBPLC grating will be increased.

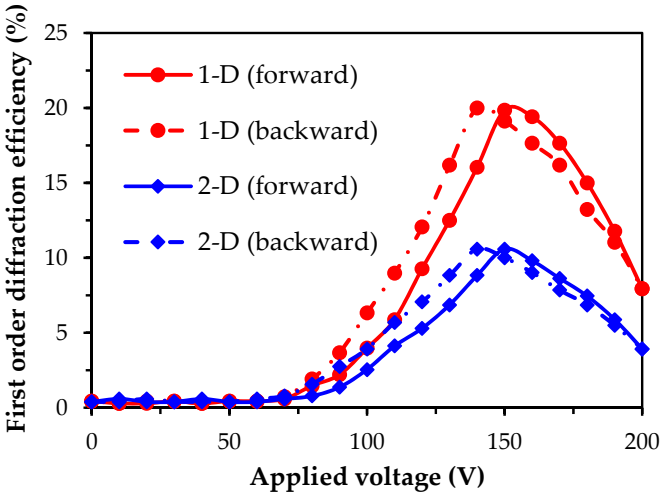


**Figure 4.** The hysteresis curves of first order diffraction efficiency for 1-D (red circle) and 2-D (blue diamond) BPLC gratings. The solid and dashed lines represent the forward and backward driving, respectively.

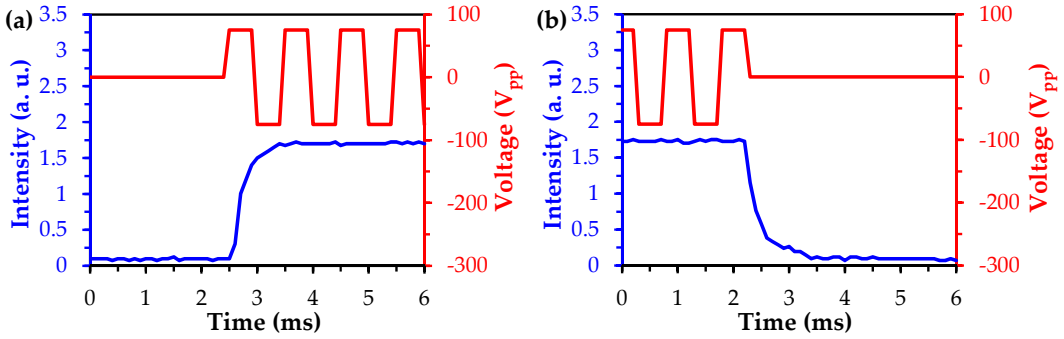


**Figure 5.** The measurement of (**a**) rise time and (**b**) decay time for the first order diffraction intensity of 1-D BPLC grating with the applied voltage switched between 0 V and 150 V.

## 3. Materials and Methods

The mixture of BPLC is prepared by nematic LC HTW114200-100 ($n_e$ = 1.779, $n_o$ = 1.513, $\Delta\varepsilon$ = +10.6 at 1 kHz, Fusol) with a weight concentration of 62.7%, and chiral dopant S811 (Fusol) with a weight concentration of 37.3%. The mixture is injected into the grating cell in the isotropic state, and then cooled from the isotropic to the blue phase by a temperature-controlled stage (LTS 120, Linkam Scientific Instruments Ltd., Tadworth, UK) at a cooling rate of 0.03 °C/min. The phase transition of the BPLC is observed using the OPM. The phase sequence of the LC phase is identified as ISO-48 °C-BPII-45.5 °C-BPI-42 °C-N*, where ISO and N* represent the isotropic phase and chiral nematic phase, respectively. The operating temperature of the BPLC grating is controlled at 45.2 °C during the experiment. The configuration of the BPLC phase grating is shown in Figure 6. The grating is composed of a BPLC layer and two glass substrates with a cell gap $d$ of 10 μm. The IPS electrode is fabricated on the bottom substrate with both the sawtooth electrode width $w$ and gap width $l$ of 20 μm by the photolithographic process. The sawtooth electrode with a turning angle of 90° is designed to achieve the effect of dimensional switching between the 1-D and 2-D phase gratings. In the $V_{off}$ state, the BPLC is optically isotropic, as shown in Figure 6a. The refractive index of BPLC is described by Equation (6):

$$n_{iso} = \frac{n_e + 2n_o}{3}. \quad (6)$$

When the voltage is applied, the direction of the LC molecule tends to be aligned with the electric field because of the positive dielectric anisotropy ($\Delta\varepsilon > 0$) of the host nematic LC. Thus, the induced optical axis of the index ellipsoid of BPLC will follow the electric field, as shown in Figure 6b. The refractive index is then changed by the electrostriction effect at the electrode gap, but remains unchanged at the center of the electrode. The difference in the refractive index between the gap of the electrodes and the center of the electrode results in the formation of the phase grating.

The experimental setup for the measurement of diffraction efficiency of the switchable two-dimensional BPLC grating is shown in Figure 7. The unpolarized He-Ne laser with a wavelength of 632.8 nm, as the probe beam, is converted into a circularly polarized beam by sequentially introducing a polarizer and a $\lambda/4$ plate. The polarization direction of linear polarized light is selected from of the circularly polarized beam with the analyzer in front of the sample. The BPLC sample is fixed on the temperature-controlled stage and applied with 1 kHz AC voltage by a power supply. A photodiode is placed behind the sample to monitor the diffraction efficiency of the BPLC grating.

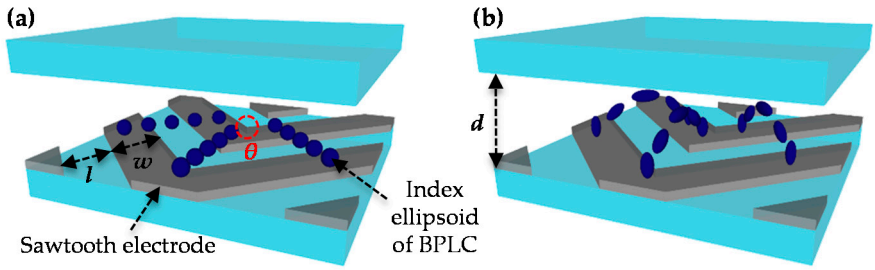


**Figure 6.** The schematic diagram of the BPLC grating in (**a**) the off state and (**b**) the on state. $w$: electrode width; $l$: electrode gap; $\theta$: turning angle; and $d$: cell gap.

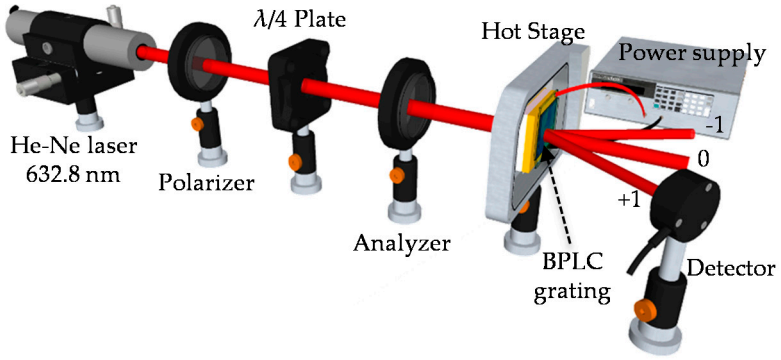


**Figure 7.** The experimental setup for the measurement of diffraction efficiency of the switchable two-dimensional BPLC grating.

## 4. Conclusions

In conclusion, switchable two-dimensional BPLC phase gratings based on a sawtooth IPS electrode have been successfully demonstrated. The dimension of the BPLC phase gratings can be switched only by changing the polarization of the incident light. According to the results, the first order diffraction efficiencies are about 20% and 10% for the 1-D and 2-D phase gratings, respectively. The hysteresis of the first order diffraction efficiency is ~10 V for 1-D and 2-D BPLC gratings, which corresponds to ~6.67% of the voltage of the maximum diffraction efficiency. The response time of the BPLC phase grating is measured to be in the sub-millisecond scale. One of the advantageous properties of our 1-D/2-D grating includes its easy dimensional interchange in response to the direction of linearly polarized light, which simultaneously fulfills both the applications of 1-D and 2-D gratings.

**Acknowledgments:** The authors would like to thank the Ministry of Science and Technology in Taiwan for financially supporting this research under Contract Nos. MOST 105-2112-M-110-004.

**Author Contributions:** Bing-Yau Huang analyzed the data and edited the manuscript; Shih-Hung Lin conceived and designed the experiments; Ke-Chin Lin performed the experiments; Chie-Tong Kuo supervised the whole study.

**Conflicts of Interest:** The authors declare no conflict of interest.

## References

1. Apter, B.; Efron, U.; Bahat-Treidel, E. On the fringing-field effect in liquid-crystal beam-steering devices. *Appl. Opt.* **2004**, *43*, 11–19. [CrossRef] [PubMed]
2. James, S.W.; Tatam, R.P. Optical fibre long-period grating sensors: Characteristics and application. *Meas. Sci. Technol.* **2003**, *14*, R49–R61. [CrossRef]
3. Fattal, D.; Peng, Z.; Tran, T.; Vo, S.; Fiorentino, M.; Brug, J.; Beausoleil, R.G. A multi-directional backlight for a wide-angle, glasses-free three-dimensional display. *Nature* **2013**, *495*, 348–351. [CrossRef] [PubMed]
4. Kang, S.W.; Chiena, L.C. Field-induced and polymer-stabilized two-dimensional cholesteric liquid crystal gratings. *Appl. Phys. Lett.* **2007**, *90*, 221110. [CrossRef]
5. Carroll, T.O. Liquid-crystal diffraction grating. *J. Appl. Phys.* **1972**, *43*, 767–770. [CrossRef]
6. Gu, L.; Chen, X.; Jiang, W.; Howley, B.; Chen, R.T. Fringing-field minimization in liquid-crystal-based high-resolution switchable gratings. *Appl. Phys. Lett.* **2005**, *87*, 201106. [CrossRef]
7. Fujieda, I. Liquid-crystal phase grating based on in-plane switching. *Appl. Opt.* **2001**, *40*, 6252–6259. [CrossRef] [PubMed]
8. Brown, C.V.; Kriezis, E.E.; Elston, S.J. Optical diffraction from a liquid crystal phase grating. *J. Appl. Phys.* **2002**, *91*, 3495–3500. [CrossRef]
9. Lindquist, R.G.; Kulick, J.H.; Nordin, G.P.; Jarem, J.M.; Kowel, S.T.; Friends, M. High-resolution liquid-crystal phase grating formed by fringing fields from interdigitated electrodes. *Opt. Lett.* **1994**, *19*, 670–672. [CrossRef] [PubMed]
10. Drevenšek-Olenika, I.; Čopič, M.; Sousa, M.E.; Crawford, G.P. Optical retardation of in-plane switched polymer dispersed liquid crystals. *J. Appl. Phys.* **2006**, *100*, 033515. [CrossRef]
11. Li, J.N.; Hu, X.K.; Wei, B.Y.; Wu, Z.J.; Ge, S.J.; Ji, W.; Hu, W.; Lu, Y.Q. Simulation and optimization of liquid crystal gratings with alternate twisted nematic and planar aligned regions. *Appl. Opt.* **2014**, *53*, E14–E18. [CrossRef] [PubMed]
12. Xu, D.; Tan, G.; Wu, S.T. Large-angle and high-efficiency tunable phase grating using fringe field switching liquid crystal. *Opt. Express* **2015**, *23*, 12274–12285. [CrossRef] [PubMed]
13. Kapoustine, V.; Kazakevith, A.; So, V.; Tam, R. Simple method of formation of switchable liquid crystal gratings by introducing periodic photoalignment pattern into liquid crystal cell. *Opt. Commun.* **2006**, *266*, 1–5. [CrossRef]
14. Hu, W.; Srivastava, A.; Xu, F.; Sun, J.T.; Lin, X.W.; Cui, H.Q.; Chigrinov, V.; Lu, Y.Q. Liquid crystal gratings based on alternate TN and PA photoalignment. *Opt. Express* **2012**, *20*, 5384–5391. [CrossRef] [PubMed]
15. Crawford, G.P.; Eakin, J.N.; Radcliffe, M.D.; Jones, A.C.; Pelcovits, P.A. Liquid-crystal diffraction gratings using polarization holography alignment techniques. *J. Appl. Phys.* **2005**, *98*, 123102. [CrossRef]
16. Provenzano, C.; Pagliusi, P.; Cipparrone, G. Electrically tunable two-dimensional liquid crystals gratings induced by polarization holography. *Opt. Express* **2007**, *15*, 5872–5878. [CrossRef] [PubMed]
17. Gao, H.; Liu, J.; Gan, F.; Ma, B. Investigation of multiple holographic recording in azo-dye-doped nematic liquid-crystal film. *Appl. Opt.* **2009**, *48*, 3014–3018. [CrossRef] [PubMed]
18. Senyuk, B.I.; Smalyukh, I.I.; Lavrentovich, O.D. Switchable two-dimensional gratings based on field-induced layer undulations in cholesteric liquid crystals. *Opt. Lett.* **2005**, *30*, 349–351. [CrossRef] [PubMed]
19. Castles, F.; Day, F.V.; Morris, S.M.; Ko, D.-H.; Gardiner, D.J.; Qasim, M.M.; Nosheen, S.; Hands, P.J.; Choi, S.S.; Friend, R.H.; et al. Blue-phase template fabrication of three-dimensional nanostructures for photonic applications. *Nat. Mater.* **2012**, *11*, 599–603. [CrossRef] [PubMed]
20. Lin, C.H.; Wang, Y.Y.; Hsieh, C.W. Polarization-independent and high-diffraction-efficiency Fresnel lenses based on blue phase liquid crystals. *Opt. Lett.* **2011**, *36*, 502–504. [CrossRef] [PubMed]
21. Ge, Z.; Gauza, S.; Jiao, M.; Xianyu, H.; Wu, S.T. Electro-optics of polymer-stabilized blue phase liquid crystal displays. *Appl. Phys. Lett.* **2009**, *94*, 101104. [CrossRef]

22. Jiao, M.; Li, Y.; Wu, S.T. Low voltage and high transmittance blue-phase liquid crystal displays with corrugated electrodes. *Appl. Phys. Lett.* **2010**, *96*, 011102. [CrossRef]
23. Kitzerow, H.S. The effect of electric field on blue phases. *Mol. Cryst. Liq. Cryst.* **1991**, *202*, 51–83. [CrossRef]
24. Yan, J.; Li, Y.; Wu, S.T. High-efficiency and fast-response tunable phase grating using a blue phase liquid crystal. *Opt. Lett.* **2011**, *36*, 1404–1406. [CrossRef] [PubMed]
25. Yan, J.; Cheng, H.C.; Gauza, S.; Li, Y.; Jiao, M.; Rao, L.; Wu, S.T. Extended Kerr effect of polymer-stabilized blue-phase liquid crystals. *Appl. Phys. Lett.* **2010**, *96*, 071105. [CrossRef]
26. Kim, M.; Kim, M.S.; Kang, B.G.; Kim, M.K.; Yoon, S.; Lee, S.H.; Ge, Z.; Rao, L.; Gauza, S.; Wu, S.T. Wall-shaped electrodes for reducing the operation voltage of polymer-stabilized blue phase liquid crystal displays. *J. Phys. D Appl. Phys.* **2009**, *42*, 235502. [CrossRef]
27. Chen, Y.; Xu, D.; Wu, S.T.; Yamamoto, S.; Haseba, Y. A low voltage and submillisecond-response polymer-stabilized blue phase liquid crystal. *Appl. Phys. Lett.* **2013**, *102*, 141116. [CrossRef]
28. Haseba, Y.; Yamamoto, S.; Sago, K.; Takata, A.; Tobata, H. Low-voltage polymer-stabilized blue-phase liquid crystals. *SID Int. Symp. Dig. Tech. Pap.* **2013**, *44*, 254–257. [CrossRef]
29. Xu, D.; Chen, Y.; Liu, Y.; Wu, S.T. Refraction effect in an in-plane-switching blue phase liquid crystal cell. *Opt. Express* **2013**, *21*, 24721–24735. [CrossRef] [PubMed]
30. Chen, K.M.; Gauza, S.; Xianyu, H.; Wu, S.T. Hysteresis effects in blue-phase liquid crystals. *J. Disp. Technol.* **2010**, *6*, 318–322. [CrossRef]
31. Nayek, P.; Jeong, H.; Kang, S.-W.; Lee, S.H.; Park, H.-S.; Lee, H.J.; Kim, H.S.; Lee, G.-D. Effect of the grain size on hysteresis of liquid-crystalline Blue Phase I. *J. Soc. Inf. Disp.* **2012**, *20*, 318–325. [CrossRef]
32. Noh, S.C.; Park, N.; Park, H.R.; Nayek, P.; Kang, S.W.; Lee, M.H.; Gong, M.-S.; Lee, S.H. Stabilizing blue phase liquid crystal with photo-reactive chiral mesogen. *SID Dig. Tech. Pap.* **2014**, *45*, 1396–1398. [CrossRef]
33. Xu, D.; Yuan, J.; Schadt, M.; Wu, S.T. Blue phase liquid crystals stabilized by linear photo-polymerization. *Appl. Phys. Lett.* **2014**, *105*, 081114. [CrossRef]
34. Liu, Y.; Xu, S.; Xu, D.; Yan, J.; Gao, Y.; Wu, S.T. A hysteresis-free polymer-stabilised blue-phase liquid crystal. *Liq. Cryst.* **2014**, *41*, 1339–1344. [CrossRef]
35. Rao, L.; Yan, J.; Wu, S.T.; Chiu, Y.H.; Chen, H.Y.; Liang, C.C.; Wu, C.M.; Hsieh, P.J.; Liu, S.H.; Cheng, K.L.; et al. Critical field for a hysteresis-free blue-phase liquid crystal device. *J. Disp. Technol.* **2011**, *7*, 627–629.
36. Hisakado, Y.; Kikuchi, H.; Nagamura, T.; Kajiyama, T. Large electro-optic Kerr effect in polymer-stabilized liquid-crystalline blue phases. *Adv. Mater.* **2005**, *17*, 96–98. [CrossRef]